Materials Research Proceedings 44 (2024) 625-634 https://doi.org/10.21741/9781644903254-67

Development of a Mg-6.8Y-2.5Zn-0.4Zr alloy (WZ73) under varying twin roll casting conditions

UEBERSCHÄR Franziska[1,a *], ULLMANN Madlen[1,b] and PRAHL Ulrich[1,c]

[1]Insititute of Metal Forming, Technische Universität Bergakademie Freiberg, Bernhard-von-Cotta-Str. 4, 09599 Freiberg, Germany

[a]franziska.ueberschaer@imf.tu-freiberg.de, [b]madlen.ullmann@imf.tu-freiberg.de, [c]ulrich.prahl@imf.tu-freiberg.de

Keywords: WZ73, Twin Roll Casting, Microstructure, Texture, LPSO

Abstract. Twin roll casting (TRC) has a big potential to produce thin strip material from magnesium alloys and enables the production in an economic manner. However, the final properties of TRC strips, such as microstructure and texture, are influenced by the twin roll casting conditions. In this work the development of a Mg-6.8Y-2.5Zn-0.4Zr alloy (WZ73) during different twin roll casting conditions, varying the twin roll casting speed, were studied. As a reference the strain and strain rate were determined. After twin roll casting the microstructure is inhomogeneous over the strip thickness and consists of a network-like structure of the LPSO phases and the α-Mg matrix. The α-Mg matrix is made up of dobulites (flake-like structures), which is already known for this alloy. [1,2] Typical defects of the twin roll cast strips were observed as well. It was also revealed that the twin roll casting conditions have a big influence on the precipitation, morphology, and phase fraction of the LPSO phases. For example, the phase fraction increases with the strain decreasing whilst the thickness of the precipitated phases increases with an increased strain. In all samples kink bands and yttrium enriched precipitations within the network like structures were detected. No dynamic recrystallization nor grain boundaries were detected. The resulting textures revealed the activation of basal slip and non-basal slip, but the intensities are small, regardless of the twin roll casting conditions.

Introduction

In recent decades, twin roll casting has become an essential method in the sheet production of light metals. This technology has proven to be especially beneficial for the fabrication of magnesium alloys. Conventional systems for forming thin strips of magnesium alloys through sheet metal involve a series of steps like continuous casting, a surface pretreatment, homogenization, pre-rolling in multiple passes, hot rolling, and multiple heat treatments. In contrast, the twin roll casting (TRC) method allows for the direct production of thin strips with thicknesses ranging from 3 to 7 mm from the molten state. This approach combines casting and rolling into a single process, making it possible to create near-net-shape semi-finished products. By leveraging the combination of TRC and strip rolling, the production of magnesium strips can be carried out in an economically and energy-efficient manner. Currently, TRC is primarily used for producing low alloy magnesium alloys like AZ31 or ZAX210. [3–6]

Over the last years magnesium alloys containing of rare earth elements became of much interest due to their good mechanical properties. [7,8] Within certain alloying systems, such as Mg-Y-Zn, the presence of Long Period Stacking Ordered (LPSO) structures significantly contributes to the enhancement of both strength and ductility. These LPSO structures exhibit a stacking sequence along the c-axis that manifests in a 10-, 14-, 18-, or 24-fold increase. [9,10] The formation of LPSO structures has been observed under various conditions, particularly in conventionally cast, heat treated, and/or hot deformed samples. [10–13]

Available literature mainly focuses on extrusion of Mg-Y-Zn alloys, different compositions or on the further processes after the initial production of sheets like the heat treatment or hot rolling. [2,14,15] Therefor in this work the focus is for the first time on the investigation of the different twin roll casting parameters and how they affect the microstructure and texture of the magnesium alloy WZ73. The investigated twin roll casting process is unique to the Institute of Metal Forming at the TU Bergakademie Freiberg.

Material and Methods

In the current study, the pilot-plant scale implementation of the horizontal TRC process was carried out using a TRC plant at an industrial scale at the Institute of Metal Forming (IMF, TU Bergakademie Freiberg). [2] The rolls had a diameter of 840 mm and were water cooled. A protective gas atmosphere was maintained while melting of the Mg-6.8Y-2.5Zn-0.4Zr (wt.%) (WZ73) magnesium alloy ingots. The chemical composition of the WZ73 alloy is provided in Table 1. The melting of WZ73 alloy ingots occurred within a steel crucible in a melting furnace, also under a protective gas atmosphere (SF_6), set at 730°C. The melting furnace was connected to a preheated launder and the adjacent nozzle through a riser. A pump facilitated the continuous supply of molten magnesium, which was then fed into the roll gap (4.5 mm) via the casting nozzle. The contact between the melt and the top and bottom rolls enabled heat transfer at the contact surfaces. Consequently, a meniscus-shaped solidification zone formed, leading to delayed solidification in the mid-section of the strip. By employing this method, it was feasible to produce a magnesium strip with a width of 710 mm and an average thickness between 5.3 mm and 5.5 mm. The TRC speed was adjusted between 1.5 and 2.1 m/min.

Table 1. Chemical composition of Mg-6.8Y-3.0Zn-0.4Zr [wt.%] alloy.

Mg [wt.%]	Y [wt.%]	Zn [wt.%]	Zr [wt.%]	Others [wt.%]
Balance	6.8	3.0	0.4	0.01

To conduct the applied equivalent strain during the twin roll casting the solidification model by Weiner et al. [16] was used. This model is based on the Freiberg Layer Model and is able to simulate the strain φ and compressed length l_d. These were then used to calculate the equivalent strain φ_v and equivalent strain rate $\dot{\varphi}_v$ via the Eq. 1 and 2 using the twin roll casting speed v_{TRC}.

$$\varphi_v = \frac{2}{\sqrt{3}} \cdot \varphi \tag{1}$$

$$\dot{\varphi}_v = \frac{v_{TRC}}{l_d} \cdot \varphi_v \tag{2}$$

Samples for microstructure analysis were prepared using traditional grinding and polishing methods. Two different acids were used for etching. In a first step a mixture of distilled water, glacial acetic acid, ethanol, and picric acid was used and for the second step nitric acid. The microstructure analysis was conducted using optical microscopy with the Keyence VHX 6000 at the IMF in Freiberg, Germany. The specimens were measured in the longitudinal direction. Additionally, a scanning electron microscope evaluation was carried out using a ZEISS GeminiSEM 450 at the same location. X-ray diffraction analysis was performed on a Seifert-FPM RD 7 instrument at the Institute of Materials Science at the TU Bergakademie Freiberg, utilizing CuKα radiation (λ = 1.540598 Å) to identify the phases. The diffraction patterns were measured within a 2θ-range of 20° to 150°, with a step size of 0.02° and a step time of 25 s. Furthermore, texture analysis was conducted using electron backscattering diffraction (EBSD) analysis on a ZEISS GeminiSEM 450 instrument at the IMF. EBSD was performed with a voltage

of 15 kV and a step size of 2.5 µm. The EBSD data was analyzed and the pole figures were calculated using the MTex MATLAB Toolbox (version 5.9.0, MTex, Ralf Hielscher, TU Bergakademie Freiberg, Germany). [17]

Results and Discussion

Calculations. For a better comparison of the different microstructures the Freiberg layer model developed by Weiner et al. [16] was used to estimate the equivalent strain φ_v and equivalent strain rate $\dot{\varphi}_v$. The results are presented in Table 2. The TRC conditions influence the strain, because due to the higher TRC speed, the material solidifies later. The reason for this is the shorter contact with the water-cooled rolls, which leads to a lower heat flow and a later material solidification. In addition, the temperature of the strip being produced is higher due to the shorter contact time with the rolls. The higher temperature delays solidification as well and provides more time for segregation processes. [18,19] A comparison of the points of solidification shows that the material solidifies approx. 10 mm closer to the roll gap outlet at the twin roll casting speed of 2.1 m/min. The subsequent solidification in return leads to a shorter compressed length and consequently a lower strain. The dependence of the strain on the TRC speed leads to the change of the equivalent strain, but the equivalent strain rate is nearly the same. Therefor for further investigation only the dependence of the equivalent strain will be considered.

Table 2. Results of the calculations based on the Freiberg layer model developed by Weiner et al. [16] regarding twin roll casting of the WZ73 alloy.

TRC speed v_{TRC} [m/min]	compressed length l_d [mm]	strain φ [-]	equivalent strain φ_v [-]	equivalent strain rate $\dot{\varphi}_v$ [s^{-1}]
1.5	46.0	0.6	0.7	0.4
1.6	44.2	0.5	0.6	0.4
2.1	38.3	0.4	0.5	0.5

Microstructure. Fig. 2 shows an overview of the microstructure over the whole strip thickness. Typical twin roll casting defects were observed and are shown in Fig. 1. For example, surface bleeds, centerline segregations, an inhomogeneous microstructure and some cracks could be detected. These are defects which have been reported before for twin roll cast WZ73 alloy and others. [19–22] The centerline segregations are the most dominant defect. It can be seen that with a decreased equivalent strain the thickness of the centerline segregation increases. This is the result of the higher deformation, the higher TRC speed and the higher temperatures of the strip as explained before. The higher speed and related phenomena lead to a bigger volume of liquid being squished into the middle, because the melt does not solidify as quickly and the contact with the rolls is shorter resulting in a lower heat rate. [18,19] The segregations observed in Fig. 2 can be described as deformation segregations. They appear due to rapid deformation process according to Lockyer et al. [23] The melt and the solid material are deformed together and small liquid regions are formed between the solid grains. [23,24] Centerline segregations in general occur due to the rapid cooling of the material which is in contact with the water-cooled rolls. The solidification front migrates towards the center of the strip which results in an alloying element enriched residual melt solidifying in the center. Furthermore, the microstructure does not consist of large dendrites which grow from the surface into the middle of the strip. These are characteristics of the microstructure observed for AZ31 or ZAX210 after twin roll casting. [4,20]

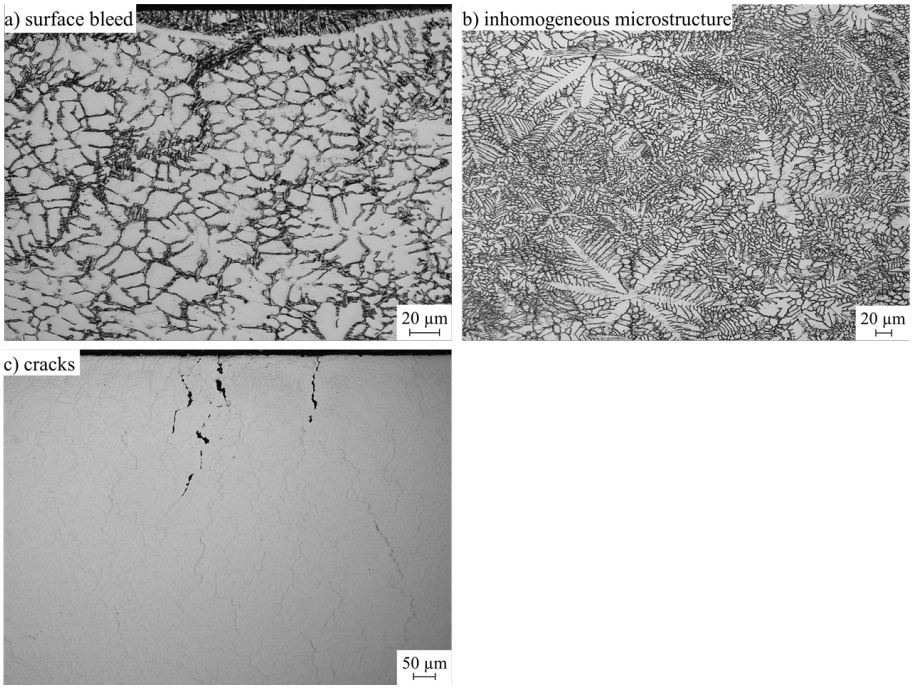

Fig. 1. Optical images of defects observed in the twin roll cast WZ73 alloy a) surface bleed; b) inhomogeneous microstructure; c) cracks.

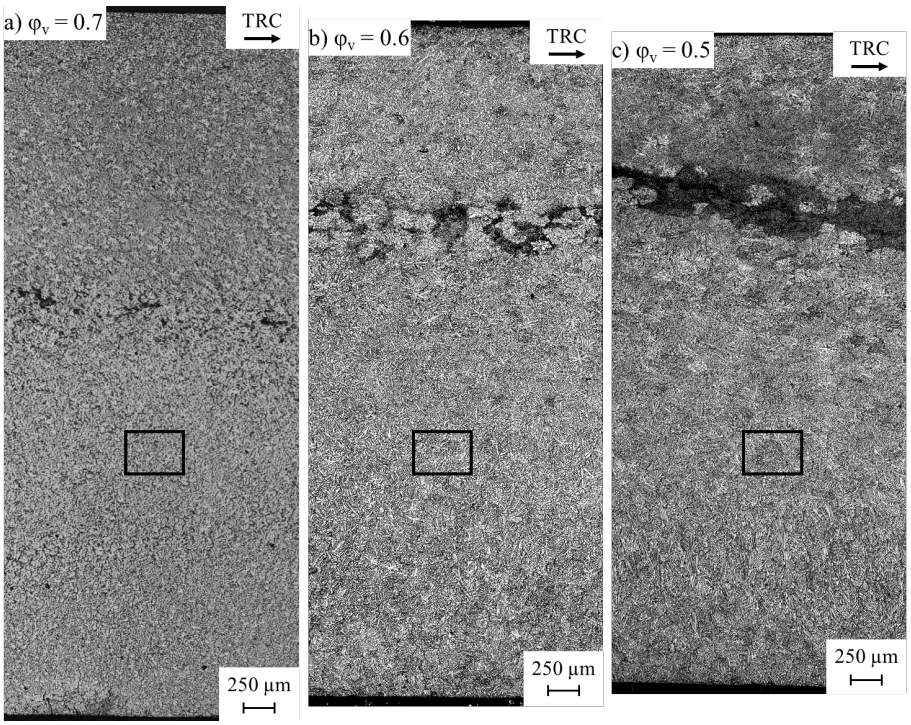

Fig. 2. Optical micrographs of the twin roll cast WZ73 alloy showing the entire strip thickness a) $\varphi_v = 0.7$; b) $\varphi_v = 0.6$ and c) $\varphi_v = 0.5$ including marked areas for Fig. 3.

Regarding the more detailed microstructure images in Fig. 3 it is visible that the microstructure consists of two parts: the α-magnesium matrix and an LPSO phase. The matrix (light parts in the optical images) is made up of dobulites (flake-like structures) whereas the LPSO phase has a network-like structure precipitated at the grain boundaries (dark parts in the optical images), which is similar to previous reported microstructure of a twin roll cast WZ73 alloy. [2,25] The phase

fraction of the LPSO phase increases slightly when the equivalent strain decreases as can be seen in Table 3. In parallel the thickness of the participated LPSO phase decreases with the equivalent strain decreasing. The increasing phase fraction is consistent with other observation in AZ31 alloys which show more precipitates when the solidification rate rises. [26] Furthermore no fine grains were detected which would indicate a dynamic recrystallisation due to the deformation process. Ullmann et al. [14] discovered that the recrystallisation behavior of the WZ73 alloy during hot rolling depends more on the equivalent strain rate than the equivalent strain. [14] The during twin roll casting applied equivalent strain rate is rather low which can be a reason for the missing sites of dynamic recrystallisation. In all samples kink bands could be identified.

Table 3. Phase fraction and thickness of the LPSO phase depending on the equivalent strain φ_v.

equivalent strain φ_v [-]	phase fraction [%]	thickness [µm]
0.7	33 ± 1.5	1.7 ± 0.7
0.6	36 ± 1.8	1.5 ± 0.7
0.5	41 ± 2.5	1.1 ± 0.4

Fig. 3b,d,f show SEM images of the twin roll cast WZ73 alloy including points of EDS measurements. In addition to the dark matrix and the LPSO phase (light grey) some white points are visible. Those were identified as yttrium rich precipitates which are too small for further identification. Other measuring points have been indicated in Fig. 3 with numbers 1 to 4. The points 1 show the α-magnesium matrix. Other yttrium and zinc rich phases have been indicated with numbers 2 and 4. The composition measured via EDS can be compared to the $Mg_{12}YZn$ phase. In previous papers this phase was noted as an LPSO phase which can be either 18R or 14H like ordered. But the precipitation along the grain boundaries indicates more likely the presence of the 18R phase. [27–29] Points 3 show zirconium rich phases. The precise composition could not be identified, because of the small size. But it can be noted, that zirconium was only found in precipitates which favorably where in the middle of dobulite structures as seen for B3 and C3. Neither in the matrix nor the in the network like structures zirconium was detected.

Table 4. Chemical composition of structural constituents according to marking in SEM images Figure 3b,d,f determined via EDS analysis (energy dispersive X-ray spectroscopy) of the twin roll cast WZ73 alloy.

		Mg [wt.%]	Y [wt.%]	Zn [wt.%]	Zr [wt.%]
$\varphi_v = 0.7$	A1	97.7	1.5	0.8	-
	A2	77.4	13.2	9.4	-
	A3	56.5	24.4	3.8	15.3
	A4	73.9	15.9	10.2	-
$\varphi_v = 0.6$	B1	98.2	1.3	0.5	-
	B2	58.7	23.3	18.0	-
	B3	61.4	29.6	1.5	7.5
	B4	80.9	12.3	6.8	-
$\varphi_v = 0.5$	C1	96.8	2.3	0.9	-
	C2	58.5	23.0	18.5	-
	C3	48.7	40.5	1.4	9.4
	C4	74.3	15.7	10.0	-

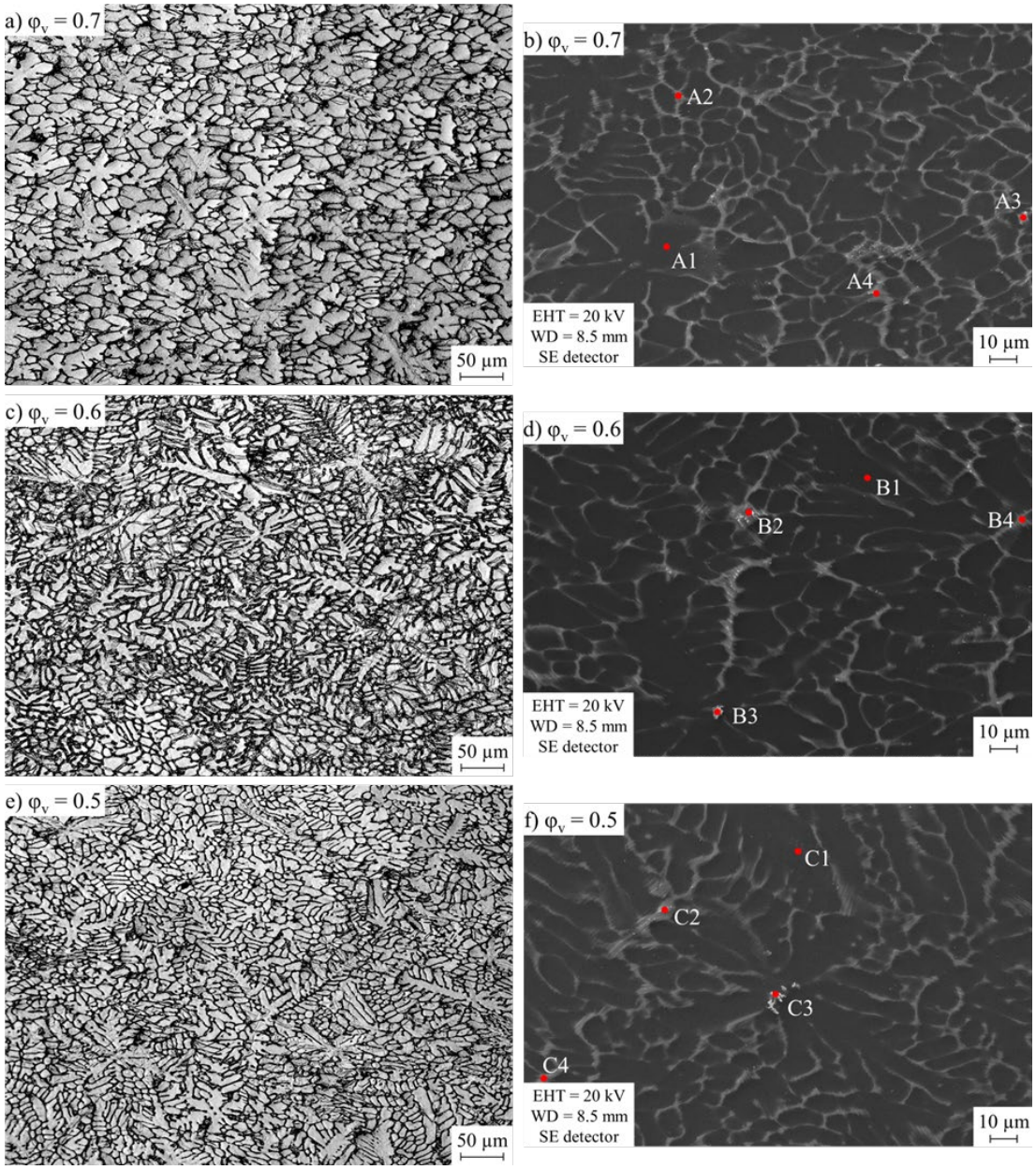

Fig. 3. Optical images (a,c,e) and SEM images (b,d,f) of the twin roll cast WZ73 (below mid-thickness as marked in Fig. 2) a,b) $\varphi_v = 0.7$; c,d) $\varphi_v = 0.6$; e,f) $\varphi_v = 0.5$ with measuring points of the EDS analysis (point 1: magnesium matrix, points 2 to 4: precipitates).

The results of the X-ray diffraction (XRD) analysis in Figure 4 show the presence of the following phases: α-Mg, $Mg_{12}YZn$, $Mg_3Y_2Zn_3$ and LPSO phases. This confirms some of the via EDS identified phases. But some of the peaks of the XRD are assigned to the $Mg_3Y_2Zn_3$ phase which usually is described as the W-phase in WZ73 alloys and has been detected in twin roll cast Mg-Y-Zn alloys before. [13,29] The little peaks at 31° and 33° are assigned to LPSO phases according to literature. [2,21,30] But a clear identification of either the 14H or 18R phase is not possible.

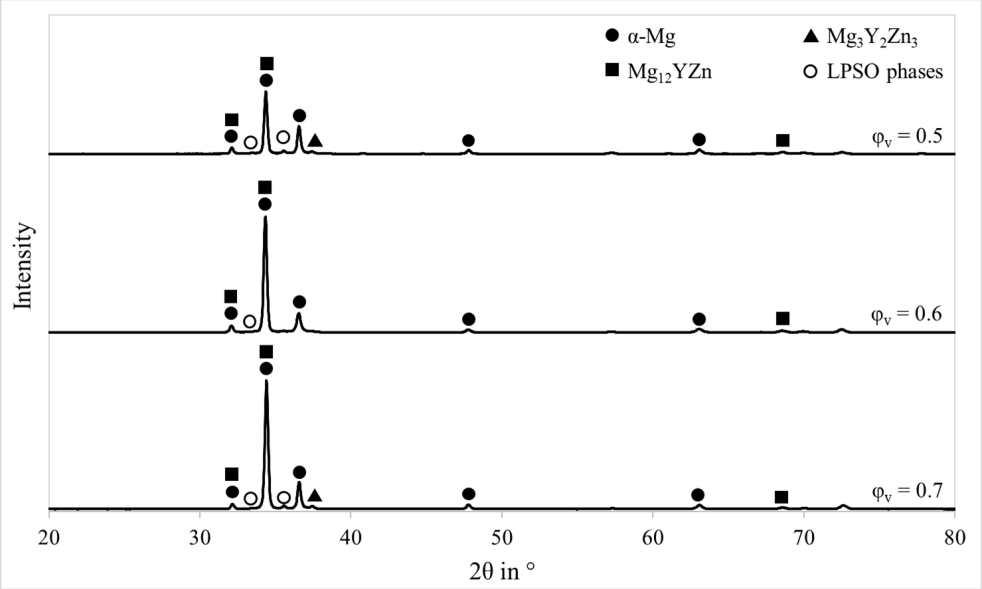

Fig. 4. Results of the XRD analysis of the twin roll cast WZ73 alloy along the cross section.

Texture. Fig. 5 shows the (0001) and (10$\bar{1}$0) pole figures of the twin roll cast WZ73 alloys (below mid thickness) depending on the different equivalent strain rates. Regardless of the equivalent strain, the pole figures show a central intensity maximum, which is slightly stretched in the transverse direction and rather low intensities. In general, however, the texture components are pronounced in the TRC direction. Only the pole figure of the samples with $\varphi_v = 0.5$ shows a second intensity maximum, which is pronounced in the twin roll cast direction. The (10$\bar{1}$0) pole figures show a so-called sixfold symmetry regardless of the equivalent strain. This symmetry and the broadened maxima of the (0001) pole figure indicate the activity of non-basal slip systems like pyramidal slip systems. This sixfold symmetry was already observed by Ullmann et al. [14] during hot rolling of WZ73 alloys. [1,14] Comparable textures were also described for twin roll cast ZAX210 or AZ31 alloys and hot rolled WE43 alloys. [4,6,31]

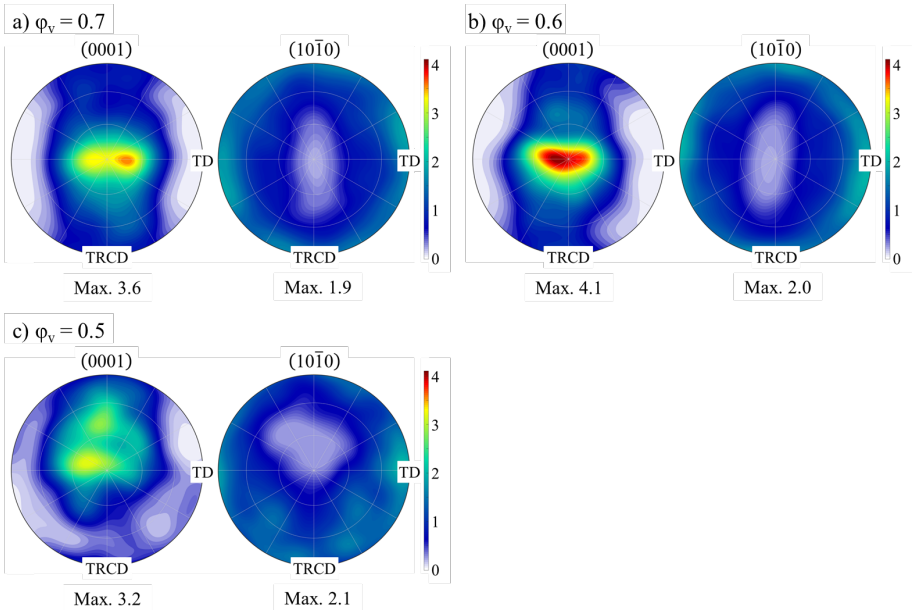

Fig. 5. (0001) and (10$\bar{1}$0) pole figure of the twin roll cast WZ73 alloy below mid-thickness a) φ_v = 0.7; b) φ_v = 0.6; c) φ_v = 0.5.

Conclusions

The present work shows the influence of twin roll casting parameters on the microstructure and texture evolution based on the equivalent strain and equivalent strain rate. The results can be summarized as follows:

1. Different TRC speeds varying from 1.5 m/min up to 2.1 m/min were tested. The solidification model was used to calculate the strain and compressed length. For all the investigated TRC speeds it was found that the equivalent strain rate is similar whilst the equivalent strain decreases with an increasing TRC speed.
2. As typical twin roll casting defects centerline segregations, an inhomogeneous microstructure, surface bleeds and cracks could be detected.
3. The microstructure consists of the α-magnesium matrix and the network-like shaped LPSO phases which participated at the grain boundaries. The phase fraction of the LPSO phases increases with the equivalent strain decreasing. The $Mg_{12}YZn$ phase could be assigned to the LPSO phase via XRD measurements. The specific ordering could not be identified clearly. But the precipitation along the grain boundaries indicate the 18R LPSO phase. Some yttrium and zirconium rich precipitates were also observed but are too small in size to clearly identify a chemical composition.
4. The texture is characterized by basal pole which is elongated in transverse direction and a low intensity. Together with the sixfold symmetry observed in the $(10\bar{1}0)$ pole figure an activation of pyramidal slip systems is indicated. Those findings are the same for all investigated equivalent strains.

Funding

This research was funded by the Deutsche Forschungsgemeinschaft (DFG, German Research Foundation) – Project number 497456843.

References

[1] M. Ullmann, K. Kittner, T. Henseler, C. Krbetschek, D. Rafaja, R. Kawalla, U. Prahl, Dynamic recrystallization and texture evolution of Mg-6.8Y-2.5Zn-0.3Zr alloy during hot rolling, Procedia Manuf. 50 (2020) 809–816. https://doi.org/10.1016/j.promfg.2020.08.146

[2] K. Kittner, M. Ullmann, F. Arndt, R. Kawalla, U. Prahl, Microstructure and Texture Evolution during Twin-Roll Casting and Annealing of a Mg–6.8Y2.5Zn–0.4Zr Alloy (WZ73), Crystals 10 (2020) 513. https://doi.org/10.3390/cryst10060513

[3] K. Neh, M. Ullmann, R. Kawalla, Twin-Roll-Casting and Hot Rolling of Magnesium Alloy WE43, Procedia Eng. (2014) 1553–1558. https://doi.org/10.1016/j.proeng.2014.10.189

[4] K. Kittner, M. Ullmann, T. Henseler, R. Kawalla, U. Prahl, Microstructure and Hot Deformation Behavior of Twin Roll Cast Mg-2Zn-1Al-0.3Ca Alloy, Materials (Basel, Switzerland) 12 (2019). https://doi.org/10.3390/ma12071020

[5] R. Kawalla, M. Ullmann, C. Schmidt, J. Dembińska, H.P. Vogt, Properties of Magnesium Strips Produced by Twin-Roll-Casting and Hot Rolling, Mater. Sci. Forum 690 (2011) 21–24. https://doi.org/10.4028/www.scientific.net/MSF.690.21

[6] G.T. Bae, J.H. Bae, D.H. Kang, H. Lee, N.J. Kim, Effect of Ca addition on microstructure of twin-roll cast AZ31 Mg alloy, Met. Mater. Int. 15 (2009) 1–5. https://doi.org/10.1007/s12540-009-0001-3

[7] Y.C. Wan, S.N. Jiang, C.M. Liu, B.Z. Wang, Z.Y. Chen, Effect of Nd and Dy on the microstructure and mechanical property of the as extruded Mg–1Zn–0.6Zr alloy, Mater. Sci. Eng. A (2015) 158–163. https://doi.org/10.1016/j.msea.2014.12.003

[8] Y.C. Wan, C. Liu, H. Xiao, Y. Gao, S. Jiang, Z.Y. Chen, Improving the Ductility of Mg-Gd-Y-Zr Alloy through Extrusion and a Following Rolling, Adv. Eng. Mater. 20 (2018) 1701041. https://doi.org/10.1002/adem.201701041

[9] A. Ono, E. Abe, T. Itoi, M. Hirohashi, M. Yamasaki, Y. Kawamura, Microstructure Evolutions of Rapidly-Solidified and Conventionally-Cast Mg97Zn1Y2 Alloys, Mater. Trans. 49 (2008) 990–994. https://doi.org/10.2320/matertrans.MC200763

[10] K. Hagihara, A. Kinoshita, Y. Sugino, M. Yamasaki, Y. Kawamura, H.Y. Yasuda, Y. Umakoshi, Effect of long-period stacking ordered phase on mechanical properties of Mg97Zn1Y2 extruded alloy, Acta Mater. 58 (2010) 6282–6293. https://doi.org/10.1016/j.actamat.2010.07.050

[11] K. Hagihara, Z. Li, M. Yamasaki, Y. Kawamura, T. Nakano, Strain-rate dependence of deformation behavior of LPSO-phases, Mater. Letters 214 (2018) 119–122. https://doi.org/10.1016/j.matlet.2017.11.117

[12] J.-B. Liu, K. Zhang, J.-T. Han, X.-G. Li, Y.-J. Li, M.-L. Ma, J.-W. Yuan, G.-L. Shi, Microstructure and texture evolution of Mg–7Y–1Nd–0.5Zr alloy sheets with different rolling temperatures, Rare Metals 39 (2020) 1273–1278. https://doi.org/10.1007/s12598-016-0740-5

[13] K.-H. Kim, J.G. Lee, G.T. Bae, J.H. Bae, N.J. Kim, Mechanical Properties and Microstructure of Twin-Roll Cast Mg-Zn-Y Alloy, Mater. Trans. 49 (2008) 980–985. https://doi.org/10.2320/matertrans.MC200752

[14] M. Ullmann, K. Kittner, U. Prahl, Hot Rolling of the Twin-Roll Cast and Homogenized Mg-6.8Y-2.5Zn (WZ73) Magnesium Alloy Containing LPSO Structures, Metals 11 (2021) 1771. https://doi.org/10.3390/met11111771

[15] K. Suzawa, S. Inoue, S. Nishimoto, S. Fuchigami, M. Yamasaki, Y. Kawamura, K. Yoshida, N. Kawabe, High-strain-rate superplasticity and tensile behavior of fine-grained Mg97Zn1Y2 alloys fabricated by chip/ribbon-consolidation, Mater. Sci. Eng. A 764 (2019) 138179. https://doi.org/10.1016/j.msea.2019.138179

[16] M. Weiner, M. Schmidtchen, U. Prahl, Extension of the Freiberg Layer Model by Means of Solidification for Roll Casting, Adv. Eng. Mater. 24 (2022). https://doi.org/10.1002/adem.202101546

[17] F. Bachmann, R. Hielscher, H. Schaeben, Texture Analysis with MTEX – Free and Open Source Software Toolbox, Semi-Solid Processing of Alloys and Composites X 160 (2010) 63–68. https://doi.org/10.4028/www.scientific.net/SSP.160.63

[18] M.A. Wells, A. Hadadzadeh, Twin Roll Casting (TRC) of Magnesium Alloys – Opportunities and Challenges, MSF 783-786 (2014) 527–533. https://doi.org/10.4028/www.scientific.net/MSF.783-786.527

[19] C. Gras, M. Meredith, J.D. Hunt, Microdefects formation during the twin-roll casting of Al–Mg–Mn aluminium alloys, J. Mater. Process. Technol. 167 (2005) 62–72. https://doi.org/10.1016/j.jmatprotec.2004.09.084

[20] A. Hadadzadeh, M.A. Wells, Inverse and centreline segregation formation in twin roll cast AZ31 magnesium alloy, Mater. Sci. Technol. 31 (2015) 1715–1726. https://doi.org/10.1179/1743284714Y.0000000750

[21] K. Kittner, M. Ullmann, F. Arndt, S. Berndorf, T. Henseler, U. Prahl, Analysis of defects in a twin roll cast Mg-Y-Zn magnesium alloy, Engineering Reports 4 (2022). https://doi.org/10.1002/eng2.12394

[22] Y. Li, C. He, J. Li, Z. Wang, Di Wu, G. Xu, A Novel Approach to Improve the Microstructure and Mechanical Properties of Al-Mg-Si Aluminum Alloys during Twin-Roll Casting, Materials (Basel, Switzerland) 13 (2020). https://doi.org/10.3390/ma13071713

[23] S.A. Lockyer, M. Yun, J.D. Hunt, D.V. Edmonds, Micro- and macrodefects in thin sheet twin-roll cast aluminum alloys, Materials Characterization 37 (1996) 301–310. https://doi.org/10.1016/S1044-5803(97)80019-8

[24] M. Yun, S. Lokyer, J.D. Hunt, Twin roll casting of aluminium alloys, Mater. Sci. Eng. A 280 (2000) 116–123. https://doi.org/10.1016/S0921-5093(99)00676-0

[25] G. Kurz, J. Wendt, J. Bohlen, D. Letzig, Microstructure Evolution of Different Magnesium Alloys During Twin Roll Casting 465–470. https://doi.org/10.1002/9781119093428.ch86

[26] A. Javaid, J. Hanke, C.H. Simha, M.S. Kozdras, Twin Roll Casting of Magnesium Strip at Canmet Materials — Modeling and Experiments, in: M.V. Manuel, A. Singh, M. Alderman, N.R. Neelameggham (Eds.), Springer eBook Collection Chemistry and Materials Science, Magnesium Technology 2015, Springer, Cham, 2016, pp. 461–464.

[27] J.F. Nie, Y.M. Zhu, A.J. Morton, On the Structure, Transformation and Deformation of Long-Period Stacking Ordered Phases in Mg-Y-Zn Alloys, Metall and Mat Trans A 45 (2014) 3338–3348. https://doi.org/10.1007/s11661-014-2301-6

[28] C. Krbetschek, R. Trân, H. Wemme, M. Ullmann, U. Prahl, D. Rafaja, Hot crack susceptibility of cast Mg 97 Y 2 Zn 1, Engineering Reports 4 (2022). https://doi.org/10.1002/eng2.12380

[29] J.Y. Yang, W.J. Kim, Effect of I(Mg3YZn6)-, W(Mg3Y2Zn3)- and LPSO(Mg12ZnY)-phases on tensile work-hardening and fracture behaviors of rolled Mg–Y–Zn alloys, J. Mater. Res. Technol. 8 (2019) 2316–2325. https://doi.org/10.1016/j.jmrt.2019.04.016

[30] M. Saadati, R.A. Khosroshahi, G. Ebrahimi, M. Jahazi, Formation of precipitates in parallel arrays on LPSO structures during hot deformation of GZ41K magnesium alloy, Mater. Charact. 131 (2017) 234–243. https://doi.org/10.1016/j.matchar.2017.07.007

[31] H. Azzeddine, D. Bradai, Texture and Microstructure of WE54 Alloy after Hot Rolling and Annealing, MSF 702-703 (2011) 453–456. https://doi.org/10.4028/www.scientific.net/MSF.702-703.453